An Approximate Solution for Laminar Boundary Layer Flow

ROBERT L. KOSSON*
Grumman Aircraft Engineering Corporation, Bethpage, N. Y.

This paper presents an approximate solution for two-dimensional, incompressible, laminar boundary layer flow with arbitrary pressure gradient. Von Mises' form of the boundary layer equation is linearized by making a change in the coefficient of one of the terms. The linearized equation yields a solution that is accurate for the outer portion of the flow but inaccurate near the surface. A separate inner solution then is developed which is accurate at the surface and which joins with the outer solution at some point within the boundary layer. The method may be considered a major modification of one developed earlier by von Kármán and Millikan, with changes in both outer and inner solutions, and the point at which the two solutions are joined. The changes improve the accuracy of the method and in some respects simplify the calculations. As examples, results are presented for flow with a linear variation of velocity (including flat plate and stagnation point flow as special cases), flow with sinusoidal variation of velocity, flow past a circular cylinder (Heimenz' velocity distribution), and flow past an ellipse (Schubauer's data). Agreement with theoretically exact solutions is good, and better than results obtained using the Pohlhausen method.

Nomenclature

A = value of velocity at joining point
a = constant (when used without subscripts)
a_m = coefficient of term in series
B = value of $\partial u/\partial y$ at joining point
b_n = coefficient of term in series
C = constant
E = value of $\partial^2 u/\partial y^2$ at joining point
f = $(u/U_a)^2$
g = total (stagnation) pressure
g_0 = total pressure in adjacent potential flow region
$g_i(\psi)$ = function representing initial boundary layer profile
k = constant or a function of x
L = reference length
M,m = integers
N,n = integers
p = pressure
$\bar{p}_i$ = mean pressure over ith increment
p_0 = pressure at origin of boundary layer ($x = 0$)
R = radius of cylinder
U_a = velocity of adjacent potential flow
U_∞ = velocity far from body
U_0 = adjacent velocity at origin of boundary layer ($x = 0$)
u = velocity component in x direction
v = velocity component in y direction
x,y = curvilinear coordinates, respectively, parallel and normal to surface
x^* = dimensionless x value [see Eq. (53)]
z = dimensionless stream function
α = defined by Eq. (17d)
Γ = standard gamma function
δ^* = displacement thickness
δ_a^*,δ_b^* = inner and linearized solution contributions, respectively, to δ^*
η = dimensionless y coordinate, or cylindrical coordinate angle
θ = momentum thickness
θ_a,θ_b = inner and linearized solution contributions, respectively, to θ
λ_n = positive constant
μ = absolute viscosity
ν = kinematic viscosity
ρ = density (constant)
τ = dummy variable for ϕ
τ_0 = shear stress at surface
ϕ = velocity potential for adjacent flow
ψ = stream function

Subscripts

e = exact value
l = linearized solution value
1 = value at joining point
∞ = value at infinity

Received by IAS October 4, 1962; revision received March 20, 1963. This paper is based on a doctoral thesis submitted to the faculty of Stevens Institute of Technology, Hoboken, N. J. The author wishes to acknowledge his indebtedness to both Robert Page, who proposed this work, and Fernando Sisto for their many suggestions during the course of this work.

* Advanced Development Group Leader, Thermodynamics and Propulsion Section. Member AIAA.

Introduction

THIS paper is concerned with one of the basic problems of fluid mechanics: steady, two-dimensional, incompressible, laminar boundary layer flow with arbitrary pressure gradient. The problem has been treated extensively by many investigators, (see, for example, Ref. 1, Chaps. 7–9 and 12, or Ref. 2, Chaps. 8–10), and some brief remarks on existing methods will be given to provide a context against which the calculation method of this paper may be considered.

A number of investigators have considered numerical solutions of the boundary layer equation of motion.[3, 4] These can be made as accurate as desired by the appropriate choice of net size, but the calculating effort involved is rather large. An alternative approach that permits theoretically "exact" solutions is the use of a series expansion for the stream functions.[5] The variables used may be chosen to make the coefficients "universal" (not related to particular body shape) functions and to minimize the number of terms required. For most problems of interest, such as flow past airfoils, the number of terms required is too large to make this method of approach practicable, however.

Because of the difficulties involved in exact solutions, a considerable amount of work has been done on approximate methods of solution. Much of this work has been on what might be called "integral methods" and uses von Kármán's momentum integral equation (an ordinary first-order differential equation) rather than Prandtl's original second-order partial differential equation of motion. In one such method developed by Pohlhausen, the velocity profile is specified as a fourth-order polynomial in powers of dimensionless distance normal to the surface, with coefficients reduced to functions of a single parameter. The value of the parameter then is found from the momentum integral equation. This method has been found satisfactory for accelerating flow but unreliable for decelerating flow. A number of alternative "single-

parameter" solutions have been proposed which provide better agreement for particular decelerating flows. There is some doubt as to the universal applicability of any of the single-parameter methods, however.

Some work also has been done on what might be called "two-parameter" solutions, involving both the momentum and energy integral equations. This is considerably more tedious (although more accurate) than the single-parameter method, since it involves the solution of two simultaneous first-order differential equations.

The integral methods all have an inherent limitation, in that the form of the velocity profile must be specified. Von Kármán and Millikan[6] developed a considerably different approximate solution using the differential boundary layer equation of motion in a form that resembles the one-dimensional heat conduction equation (von Mises' transformation). The equation is reduced to two more simple (linearized) forms, one valid near the outer edge of the boundary layer and the other valid near the surface. These equations yield two solutions (termed "outer" and "inner"). The inner solution is used only for decelerating flow and is applied to the region between the surface and the velocity profile inflection point. The outer solution is applied to the entire flowfield for accelerating flow and to the region between the inflection point and the outer edge of the boundary layer for decelerating flow. The method has been applied to a few cases only. Although it seems to be more reliable than the Pohlhausen method in predicting separation, it errs in setting the separation point too far forward and in predicting too rapid a boundary layer growth.

The method presented in this paper follows an approach similar to that of von Kármán-Millikan described in the foregoing and may be considered a major modification of it. It differs from that of von Kármán-Millikan in a number of respects. The outer solution contains a constant coefficient (less than unity) applied to some of the terms and is presented in a form permitting more direct use of pressure distribution data. An inner solution is used at all times and is one of two forms. For highly inflected velocity profiles near the point of flow separation, the original von Kármán-Millikan inner solution is retained, except for a slight change to accommodate the revised outer solution. For all other cases, a fourth-order polynomial velocity profile is used, with coefficients determined from boundary conditions at the surface and properties of the outer solution where the two solutions join. The joining point is no longer the velocity profile inflection point. In addition to these differences, the notation used is quite different from (and hopefully simpler than) that of von Kármán-Millikan. The resulting method is more accurate than that of von Kármán-Millikan and, in some respects, easier to apply.

With respect to other boundary layer calculation procedures, the method presented in this paper occupies a middle ground between the single-parameter integral methods and the numerical solutions from the point of view of both accuracy and ease of calculation.

Basic Equations and Boundary Conditions

For steady laminar two-dimensional incompressible flow, Prandtl's boundary layer equation of motion in the direction of flow is

$$u\frac{\partial u}{\partial x} + v\frac{\partial u}{\partial y} = -\frac{1}{\rho}\frac{dp}{dx} + \nu\frac{\partial^2 u}{\partial y^2} \tag{1}$$

and the continuity equation is

$$(\partial u/\partial x) + (\partial v/\partial y) = 0 \tag{2}$$

Boundary conditions are

$$y = 0 \qquad u = 0 \qquad v = 0 \tag{3a}$$

$$y = \infty \qquad u = U_a \tag{3b}$$

In addition, there is an initial (boundary) condition:

$$x = 0 \qquad u = u_i(y) \tag{3c}$$

where $u_i(y)$ is the initial boundary layer velocity profile.

Applying these boundary conditions to Eqs. (1) and (2), certain additional relationships may be obtained which will be satisfied by any exact solution.

At $y = 0$,

$$\nu(\partial^2 u/\partial y^2) = (1/\rho)(dp/dx) \tag{4a}$$

$$\nu(\partial^3 u/\partial y^3) = 0 \tag{4b}$$

$$\nu(\partial^4 u/\partial y^4) = (\partial u/\partial y)(\partial^2 u/\partial y \partial x) \text{ etc.} \tag{4c}$$

and at $y = \infty$,

$$\partial^n u/\partial y^n = 0 \qquad n = 1, 2, 3, \ldots \tag{4d}$$

These relations are termed compatibility conditions. They frequently are considered as additional boundary conditions in dealing with approximate solutions of the boundary layer equations and will be considered as such in this paper. In general, approximate solutions satisfy the original boundary conditions [Eq. (3)] and some, but not all, of the compatibility conditions.

The boundary layer equations can be put into a much simpler form by the use of a transformation first published by R. von Mises in 1927 (discussed in Ref. 1, Chap. 8).

A stream function ψ is defined by

$$u = \partial\psi/\partial y \qquad v = -\partial\psi/\partial x \tag{5}$$

This satisfies the continuity Eq. (2).

A velocity potential ϕ is defined by

$$\phi = \int_0^x U_a dx \tag{6}$$

where U_a is the velocity of the adjacent inviscid flow. Also, a total pressure g is defined by

$$g = p + \tfrac{1}{2}\rho(u^2 + v^2) \tag{7}$$

Consistent with the boundary layer assumption that $v \ll u$, Eq. (7) may be written as

$$g = p + \tfrac{1}{2}\rho u^2 \tag{7a}$$

Using ϕ and ψ as independent variables and g as a dependent variable, Prandtl's boundary layer equation of motion (1) becomes

$$\partial g/\partial\phi = \nu(u/U_a)(\partial^2 g/\partial\psi^2) \tag{8}$$

where

$$u/U_a = [(2/\rho U_a^2)(g - p)]^{1/2} \tag{9}$$

and the boundary conditions (3) become

$$\psi = 0 \qquad g = p \tag{10a}$$

$$\psi = \infty \qquad g = g_0 \tag{10b}$$

$$\phi = 0 \qquad g = g_i(\psi) \tag{10c}$$

where g_0 is the total pressure outside the boundary layer, and $g_i(\psi)$ the initial boundary layer total pressure profile.

One advantage in using g as the dependent variable is that the effect of variation in pressure shows up in the boundary condition at $\psi = 0$ rather than at $\psi = \infty$. On the debit side, however, it may be noted that Eq. (8) has a singularity at the wall for the general case of varying pressure. For $\psi = 0$, the left-hand side of Eq. (8) becomes

$$\partial g/\partial\phi = dp/d\phi \neq 0$$

For the right-hand side, since $u/U_a = 0$ at $\psi = 0$, one must have

$$\partial^2 g/\partial\psi^2 = \infty$$

Following a technique used by Nash[7] and Lewis and Carrier,[13] the ratio (u/U_a) appearing as a coefficient in Eq. (8) is replaced by a positive constant C, less than unity, giving

$$\partial g/\partial \phi = C\nu(\partial^2 g/\partial \psi^2) \tag{11}$$

This is a linear equation, equivalent to the one-dimensional heat conduction equation.

For $C = 1$, Eq. (11) is equivalent to that used by von Kármán and Millikan[6] for their outer solution. The value of C may be established by a variety of averaging processes, most of which indicate a value in the neighborhood of 0.8.

It should be noted that any value of $C > 0$ eliminates the singularity in the differential equation at $\psi = 0$ and hence changes the nature of the solution at the surface. In particular, for $\psi = 0$, Eq. (11) gives

$$\partial^2 g/\partial \psi^2 = (1/C\nu)(dp/dx)$$

which is finite. This is equivalent to getting

$$\partial^2 u/\partial y^2 = (u/\rho)(\partial^2 g/\partial \psi^2) = 0 \qquad \text{at } y = 0$$

rather than the correct value indicated by Eq. (4a).

Because of the changes introduced near the surface, the solution of Eq. (11) is applied only to the outer portion of the boundary layer flow, and a separate inner solution is developed for the flow immediately adjacent to the surface. The two solutions will be discussed separately.

Outer Solution

Equation (11) with boundary conditions [Eqs. (10a–10c)] is analogous to a one-dimensional heat conduction problem (semi-infinite slab with specified initial temperature distribution and time-dependent surface temperature), the solution of which is given in Ref. 8, Chap. 2 or other texts on the theory of heat conduction in solids.

The solution, for any initial boundary layer profile $g_i(\psi)$ and any pressure gradient $p(\phi)$, may be written as

$$g = \frac{1}{2(\pi C\nu\phi)^{1/2}} \int_0^\infty g_i(\psi)\left[e^{-(\zeta-\psi)^2/4C\nu\phi} - e^{-(\zeta+\psi)^2/4C\nu\phi}\right] \times d\zeta + p(\phi) - p_0 \operatorname{erf}\left[\frac{\psi}{2(C\nu\phi)^{1/2}}\right] - \int_0^\phi \frac{dp(\tau)}{d\tau} \operatorname{erf}\left(\frac{\psi}{2[C\nu(\phi-\tau)]^{1/2}}\right) d\tau \tag{12}$$

where ζ and τ are dummy variables for integrations over ψ and ϕ, respectively, and erf denotes the error function, defined by

$$\operatorname{erf}(z) = \frac{2}{(\pi)^{1/2}} \int_0^z e^{-\beta^2} d\beta$$

For the special case $g_i(\psi) = g_0$, corresponding to zero initial boundary layer thickness, Eq. (12) simplifies to

$$g = g_0 \operatorname{erf}\left[\frac{\psi}{2(C\nu\phi)^{1/2}}\right] + \frac{\psi}{2(\pi C\nu)^{1/2}} \int_0^\phi p(\tau) \frac{\exp[-\psi^2/4C\nu(\phi-\tau)]}{(\phi-\tau)^{3/2}} d\tau \tag{13}$$

One feature of Eq. (13) which might be noted is that the solution is a function of the dimensionless group

$$z = \psi/2(C\nu\phi)^{1/2} \tag{14}$$

In terms of z, Eq. (13) becomes

$$g - g_0 \operatorname{erf} z = \frac{z}{\phi(\pi)^{1/2}} \int_0^\phi p(\tau) \frac{\exp[-z^2/(1-\tau/\phi)]}{(1-\tau/\phi)^{3/2}} d\tau \tag{15}$$

The integral in Eq. (15) can be evaluated in terms of standard functions for a number of particular choices of $p(\phi)$. For example, if $p(\phi)$ can be approximated by all or part of the expression

$$p(\phi) = \sum_{m=0}^{M} a_m \phi^{m/2} + \sum_{n=0}^{N} b_n e^{\lambda_n \phi} \tag{16}$$

where m, n are integers, and $\lambda_n > 0$, then the solution is

$$g - g_0 \operatorname{erf} z = \sum_{m=0}^{M} a_m \Gamma\left(\frac{m}{2}+1\right)(4\phi)^{m/2}\, i^m\operatorname{erfc} z + \sum_{n=0}^{N} \frac{b_n e^{\lambda_n\phi}}{2}\{\exp[-2z(\lambda_n\phi)^{1/2}] \operatorname{erfc}[z-(\lambda_n\phi)^{1/2}] + \exp[+2z(\lambda_n\phi)^{1/2}] \operatorname{erfc}[z+(\lambda_n\phi)^{1/2}]\} \tag{17}$$

where Γ is the standard gamma function:

$$\Gamma(n) = \int_0^\infty e^{-\beta}\, \beta^{n-1} d\beta \tag{17a}$$

and $i^m\operatorname{erfc} z$ is the mth repeated integral of the complementary error function:

$$i^m\operatorname{erfc} z \equiv \int_z^\infty i^{m-1}\operatorname{erfc}\beta\, d\beta \tag{17b}$$

with

$$i^0\operatorname{erfc} z \equiv \operatorname{erfc} z \equiv \frac{2}{(\pi)^{1/2}} \int_z^\infty e^{-\beta^2} d\beta \tag{17c}$$

Values of $i^m\operatorname{erfc} z$ are tabulated in Ref. 8.

This is essentially the approach followed by von Kármán and Millikan (setting $b_n = 0$ and taking even values of m). Considerable care must be exercised in obtaining the proper expression for pressure as a function of velocity potential [Eq. (16)] for problems involving flow separation,[9] and, once obtained, a considerable amount of algebra is involved to actually obtain the solution.

For most problems, if only a limited amount of information about the boundary layer is desired, or if a digital computer is to be used, a numerical evaluation of the integral in Eq. (15) probably will prove most convenient. In making a numerical evaluation, it may be noted that the integrand remains bounded for all values of τ but varies rapidly with τ in the vicinity of $\tau = \phi$.

An approach that avoids this difficulty is to divide the surface of the body into N increments (not necessarily equal), on each of which the pressure may be assumed constant. Let x_i and τ_i denote the distance coordinate and velocity potential at the end of the ith increment, and $\bar{p}_i$ the mean pressure on this increment. Then, introducing a new dummy variable,

$$\alpha(\tau) \equiv \frac{z}{(1-\tau/\phi)^{1/2}} \tag{17d}$$

Eq. (15) becomes

$$g - \{g_0 \operatorname{erf} z = \sum_{i=1}^{N} \bar{p}_i \frac{2}{(\pi)^{1/2}} \int_{\alpha_{i-1}}^{\alpha_i} e^{-\alpha^2} d\alpha \tag{18}$$

Evaluating the integral and substituting for g with Eq. (7a) gives

$$u^2 = \frac{2}{\rho}\left\{ g_0 \operatorname{erf} z - p + \sum_{i=1}^{N} \bar{p}_i[\operatorname{erf}(\alpha_i) - \operatorname{erf}(\alpha_{i-1})]\right\} \tag{19}$$

where $\alpha_i \equiv \alpha(\tau_i)$.

Equation (19) gives the velocity at specified values of $z > 0$ [defined by Eq. (14)] and x. As stated earlier, this solution should not be used for very small values of z because of the approximations introduced in the original differential Eq. (11).

Alternative expressions, both more accurate and more complicated than (19), can be developed by assuming a form of pressure variation within each increment which permits the integral in Eq. (15) to be evaluated in closed form over the increment. Equation (19) actually was used in most of the numerical calculations, but no attempt was made to optimize the calculation procedure.

Equations (15, 17, and 19) give values of g (or u) as a function of z. The corresponding y values may be obtained, applying Eqs. (5) and (14), from

$$y = y_1 + 2(C\nu\phi)^{1/2} \int_{z_1}^{z} \frac{dz}{u} \tag{20}$$

where subscript 1 denotes values at the joining point of the inner and outer solutions. The value of y_1 is determined from the inner solution, discussed in a following section, and the outer solution is applied only for values of $y \geq y_1$, $z \geq z_1$.

Evaluation of "C"

In altering von Mises' form of the boundary layer Eq. (8) to a linear form [Eq. (11)], the author had set

$$\nu(u/U_a)(\partial^2 g/\partial\psi^2) \approx C\nu(\partial^2 g/\partial\psi^2) \tag{21}$$

This is equivalent to setting

$$\partial^2 u_e/\partial y^2 \approx C(U_a/u_l)(\partial^2 u_l/\partial y^2) \tag{22}$$

where subscripts e and l denote exact and linearized equations, respectively. From relation (22) one might expect the quantity $C(U_a/u)(\partial^2 u/\partial y^2)$, as determined from the linearized solution, to be approximately equal to the exact solution value of $\partial^2 u/\partial y^2$. A check on this expectation was made for the case of flow on a flat plate, using the Blasius solution for the exact values of $\partial^2 u/\partial y^2$. Comparing at equal values of velocity, the two quantities were found to agree within approximately 8%, as shown in Fig. 1.

Multiplying relation (22) by dy and integrating over the region of applicability of the outer solution,

$$-\left.\frac{\partial u_e}{\partial y}\right|_{y=y_1} \approx CU_a \int_{y_1}^{\infty} \frac{1}{u_l}\frac{\partial^2 u_l}{\partial y^2}\, dy \tag{23}$$

Hence, if one wants an approximately correct value of $\partial u/\partial y\,|_{y=y_1}$ for the linearized solution, one should choose C such that

$$-\left.\frac{\partial u}{\partial y}\right|_{y=y_1} = CU_a \int_{y_1}^{\infty} \frac{1}{u}\frac{\partial^2 u}{\partial y^2}\, dy \tag{24}$$

where the subscripts have been dropped since all quantities are evaluated using the linearized solution.

Introducing $f(\phi,z)$ defined by

$$f = (u/U_a)^2 = (g - p)/(g_0 - p) \tag{25}$$

one may write Eq. (24) in terms of f and z as

$$C = -\left[\left.\frac{\partial f}{\partial z}\right|_{z=z_1} \Big/ \int_{z_1}^{\infty} \frac{1}{(f)^{1/2}}\frac{\partial^2 f}{\partial z^2}\, dz\right] \tag{26}$$

The value of C determined from Eq. (26) is dependent on the value of z_1 selected and to a lesser extent on the value of ϕ (or x) at which the calculation is made. Although no general rule can be given for determining the "best" values of z_1 and ϕ for each particular problem, good results have been obtained using $z_1 = 0.15$ and a value of ϕ near the upstream end of the boundary layer. In general, the values of C determined in this way are within a few percent of 0.8.

Inner Solution

There are many approaches that might be used to arrive at an inner solution for the boundary layer flow. The inner solution must, of course, satisfy the boundary condition

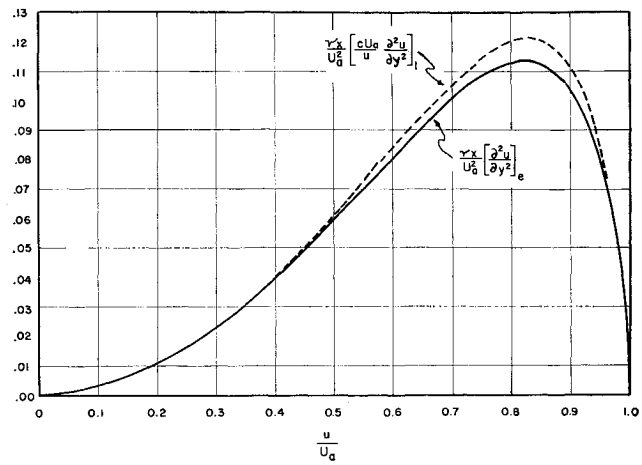

Fig. 1 Comparison of terms in relation (22) for flow on a flat plate; $dp/dx = 0$

$u = 0$ at $y = 0$. Also, if it is to represent an improvement over the outer solution at $y = 0$, it should satisfy the compatibility condition (4a) for $\partial^2 u/\partial y^2$ and as many additional compatibility conditions as possible.

At the joining point, the inner solution should have the same velocity and normal velocity gradient $\partial u/\partial y$ as the outer solution. The second derivatives should not be equated, since, as discussed in the preceding section, a better estimate of the correct value is given by

$$\partial^2 u/\partial y^2 = C(U_a/u_l)(\partial^2 u_l/\partial y^2) \tag{27}$$

where subscript l again denotes the outer (linearized) solution.

Von Kármán and Millikan[3] investigated methods of simplifying the boundary layer equation using approximations that would be valid at $y = 0$. The inner solution finally proposed by them is restricted to velocity profiles having an inflection point (primarily regions of decelerating flow) and uses the inflection point as the joining point of the inner and outer solutions. The inner solution uses an approximation equivalent to setting

$$\left.\frac{\partial u}{\partial x}\right|_{\psi=\text{const}} = -\frac{1}{\rho A}\frac{dp}{dx} \tag{28}$$

where A is the velocity at the inflection point ($\partial^2 u/\partial y^2 = 0$).

With this approximation, the boundary layer Eq. (1) becomes

$$(\partial^2 u/\partial y^2) + (k/A)u = k \tag{29}$$

where

$$k = k(x) = \frac{1}{\rho\nu}\frac{dp}{dx} = -\frac{U_a}{\nu}\frac{dU_a}{dx}$$

Equation (29) then is solved as an ordinary second-order linear differential equation in y using the following boundary conditions:

$$y = 0 \qquad u = 0, \qquad \text{hence } \partial^2 u/\partial y^2 = (1/\rho\nu)(dp/dx) \tag{30a}$$

$$y = y_1 \qquad u = A, \qquad \text{hence } \partial^2 u/\partial y^2 = 0 \tag{30b}$$

$$y = y_1 \qquad \partial u/\partial y = \partial u/\partial y\,|_{y=y_1} \equiv B \tag{30c}$$

Three boundary conditions are used because y_1 is unspecified. The solution of (29) may be written as

$$u = A - B(A/k)^{1/2} \sin\{(k/A)^{1/2}(y_1 - y)\} \tag{31}$$

where

$$y_1 = (A/k)^{1/2} \sin^{-1}\{(Ak)^{1/2}/B\} \tag{32}$$

This is equivalent to the inner solution obtained by von Kármán and Millikan but in a somewhat different form. The principal drawbacks to this inner solution are that it cannot be used for accelerating flow (where there is no inflection point in the velocity profile), and it leads to inaccuracy in the outer solution when the inflection point is close to the surface. The solution is best suited for use near the point of flow separation, where the inflection point is far from the surface. Also, at the separation point, it can be shown that this inner solution satisfies the additional compatibility condition, $\partial^3 u/\partial y^3 = 0$.

An alternate inner solution that avoids the drawbacks of the von Kármán-Millikan inner solution can be obtained by approximating the velocity profile with a fourth-order polynomial of the form

$$u = a_0 + a_1 y + a_2 y^2 + a_3 y^3 + a_4 y^4 \tag{33}$$

and using the boundary conditions

$$y = 0 \qquad u = 0 \tag{34a}$$

$$y = 0 \qquad \partial^2 u/\partial y^2 = (1/\rho\nu)(dp/dx) \tag{34b}$$

$$y = 0 \qquad \partial^3 u/\partial y^3 = 0 \tag{34c}$$

$$y = y_1 \qquad u = A \tag{34d}$$

$$y = y_1 \qquad \partial u/\partial y = B \tag{34e}$$

$$y = y_1 \qquad \partial^2 u/\partial y^2 = (CU_a/A)(\partial^2 u/\partial y^2)\,|_{y=y_1} \equiv E \tag{34f}$$

Six boundary conditions are used, since there are six unknowns (five coefficients and y_1).

Applying Eqs. (34) gives

$$a_0 = a_3 = 0 \tag{35a}$$

$$a_2 = (1/2\rho\nu)(dp/dx) \tag{35b}$$

$$y_1 = [2B/(E + 2a_2)]\{1 - [1 - (A/B^2)(E + 2a_2)]^{1/2}\} \tag{35c}$$

$$a_1 = B - (y_1/3)(E + 4a_2) \tag{35d}$$

$$a_4 = (E - 2a_2)/12y_1^2 \tag{35e}$$

The values A,B, and E are determined from the outer solution at the specified value of z_1 and the desired value of ϕ (or x). Since the outer solution is expressed most easily in terms of $f(\phi,z) \equiv (u/U_a)^2$, it is convenient to evaluate A, B, and E in the form

$$A = U_a(f_1)^{1/2} \tag{36a}$$

$$B = [U_a^2/4(C\nu\phi)^{1/2}](\partial f/\partial z)\,|_{z=z_1} \tag{36b}$$

$$E = (U_a^3/8\nu\phi)(\partial^2 f/\partial z^2)\,|_{z=z_1} \tag{36c}$$

where $f_1 \equiv f(\phi,z_1)$.

For numerical evaluation, combining Eqs. (19) and (36a–36c) gives

$$A^2 = \frac{2}{\rho}\left\{g_0 \mathrm{erf} z_1 - p + \sum_{i=1}^{N} \bar{p}_i[\mathrm{erf}(\alpha_i) - \mathrm{erf}(\alpha_{i-1})]\right\} \tag{37a}$$

$$B = \frac{1}{\rho(C\nu\phi\pi)^{1/2}}\left\{g_0 e^{-z_1^2} + \frac{1}{z_1}\sum_{i=1}^{N} \bar{p}_i[\alpha_1 e^{-\alpha_i^2} - \alpha_{i-1} e^{-\alpha_{i-1}^2}]\right\} \tag{37b}$$

$$E = -\frac{U_a}{\rho\nu\phi(\pi)^{1/2}}\left\{g_0 z_1 e^{-z_1^2} + \frac{1}{z_1^2}\sum_{i=1}^{N} \bar{p}_i[\alpha_i^3 e^{-\alpha_i^2} - \alpha_{i-1}^3 e^{-\alpha_{i-1}^2}]\right\} \tag{37c}$$

With respect to the choice of boundary conditions, it may be noted that one additional boundary condition (34c) has been applied compared with the von Kármán-Millikan inner solution. The remaining boundary conditions are the same, except that $\partial^2 u/\partial y^2$ is not equal to zero at $y = y_1$, since y_1 is not necessarily an inflection point.

Of the two solutions, the polynomial inner solution is the easier to apply, since there is no necessity of first determining the velocity profile inflection point for the outer solution. Also, because of the additional boundary condition (34c), the polynomial solution is the more accurate of the two, except in the region near the separation point. Near the separation point, however, the polynomial solution is found to be less accurate than the von Kármán-Millikan solution. In part, this reflects the increased accuracy of the von Kármán-Millikan inner solution in this region [satisfying boundary condition (34c) at the separation point], but also the assumed polynomial form for the velocity profile becomes less accurate as the extent of the region covered by the inner solution ($0 \leq y \leq y_1$) increases.

For the calculations reported in this paper, the polynomial inner solution has been used with $z_1 = 0.15$, excepting cases where the outer solution had a velocity profile inflection point at $z > 0.15$, when the von Kármán-Millikan inner solution was used. This criterion is found to provide reasonably good results, as will be shown in the examples that follow. Some further refinement in choice of z_1 and selection of inner solution probably can be made, however.

Combined Inner and Outer Solutions

The quantities of particular interest in boundary layer calculations are the shear stress at the surface, displacement thickness, and momentum thickness. Equations for determining these quantities follow.

Shear Stress τ_0

From the definition of viscosity

$$\tau_0 = \mu(\partial u/\partial y)\,|_{y=0} = \rho\nu(\partial u/\partial y)\,|_{y=0} \tag{38}$$

For the polynomial inner solution,

$$\tau_0 = \rho\nu a_1 \tag{39}$$

where a_1 is given by (35d).

For the von Kármán-Millikan inner solution,

$$\tau_0 = \rho\nu B \cos\{(k/A)^{1/2}(y_1 - y)\} \tag{40}$$

where y_1 is given by (32).

Displacement Thickness δ^*

The contributions of the inner and outer solutions must be evaluated separately in calculating the displacement thickness:

$$\delta^* = \delta_a^* + \delta_b^* \tag{41}$$

where

$$\delta_a^* \equiv \int_0^{y_1}\left(1 - \frac{u}{U_a}\right)dy \tag{42}$$

$$\delta_b^* \equiv \int_{y_1}^{\infty}\left(1 - \frac{u}{U_a}\right)dy \tag{43}$$

For the polynomial inner solution, substituting Eqs. (33) and (35) in (42) gives

$$\delta_a^* = y_1\left[1 - \frac{1}{2}\left(\frac{A}{U_a}\right)^{1/2} + \frac{y_1^2}{U_a}\left(\frac{3E + 14a_2}{120}\right)\right] \tag{44}$$

where y_1 is given by (35c).

For the von Kármán-Millikan inner solution, substituting Eq. (31) in (42) gives

$$\delta_a^* = \left(1 - \frac{A}{U_a}\right)y_1 + \frac{BA}{U_a k}\left[1 - \cos\left(\frac{k}{A}\right)^{1/2} y_1\right] \tag{45}$$

where y_1 is given by (32).

For the outer solution, Eq. (43) may be expressed in terms of z as

$$\delta_b^* = \frac{2(C\nu\phi)^{1/2}}{U_a}\int_{z_1}^{\infty}\left(\frac{U_a}{u}-1\right)dz \tag{46}$$

The integral, in general, must be evaluated numerically using values of u obtained from (7a) and (17) or from (19).

Momentum Thickness θ^*

The momentum thickness also must be evaluated in two parts. One may write

$$\theta = \theta_a + \theta_b \tag{47}$$

where

$$\theta_a \equiv \int_0^{y_1}\left(\frac{u}{U_a}\right)\left(1-\frac{u}{U_a}\right)dy \tag{48}$$

and

$$\theta_b \equiv \int_{y_1}^{\infty}\left(\frac{u}{U_a}\right)\left(1-\frac{u}{U_a}\right)dy \tag{49}$$

For the polynomial inner solution, substituting Eqs. (33) and (35) in (48) gives

$$\theta_a = \frac{y_1^2}{U_a}\left\{\frac{a_1U_a}{2}+\frac{y_1}{3}(a_2U_a-a_1^2)-\frac{y_1^4}{4}(2a_1a_2)+\right.$$
$$\left.\frac{y_1^3}{5}(a_4U_a-a_2^2)-\frac{y_1^4}{6}(2a_1a_4)-\frac{y_1^5}{7}(2a_2a_4)-\frac{y_1^7}{9}a_4^2\right\} \tag{50}$$

where y_1 is given by (35c).

For the von Kármán-Millikan inner solution, substituting Eq. (31) in (48) gives

$$\theta_a = \frac{y_1}{U_a^2}A(U_a-A)+\frac{BA}{U_a^2k}\left\{2A-U_a-\frac{By_1}{2}+\right.$$
$$\left.(U_a-\frac{3}{2}A)\cos\left(\frac{k}{A}\right)^{1/2}y_1\right\} \tag{51}$$

where y_1 is given by (32).

For the outer solution, Eq. (49) may be expressed in terms of z as

$$\theta_b = \frac{2(C\nu\phi)^{1/2}}{U_a}\int_{z_1}^{\infty}\left(1-\frac{u}{U_a}\right)dz \tag{52}$$

As with δ_b^*, the integral, in general, must be evaluated numerically, using values of u obtained from (7a) and (17) or from (19).

Applications of the Method

To test the method, calculations have been made for a number of flow problems for which either theoretically exact solutions or experimental data are available. Four cases that will be presented are 1) linear variation in velocity (including flat plate and two-dimensional stagnation point flow as special cases); 2) sinusoidal variation in velocity; 3) circular cylinder (Hiemenz velocity distribution); and 4) Schubauer's ellipse.

These examples include both accelerating and decelerating flows, and flows from stagnation point to separation point. They will be discussed separately below.

Linear Variation in Velocity

Consider the case

$$U_a = U_0 + ax = U_0(1+x^*) \tag{53}$$

where U_0 is the initial stream velocity, a is a constant (positive or negative), and $x^* \equiv ax/U_0$.

Table 1 Results for linear variation of velocity

x^*	$\frac{\tau_0}{\rho U_0(\lvert a\rvert\nu)^{1/2}}$ Approx.	Exact	$\delta^*\left(\frac{\lvert a\rvert}{\nu}\right)^{1/2}$ Approx.	Exact	$\theta\left(\frac{\lvert a\rvert}{\nu}\right)^{1/2}$ Approx.	Exact
Decelerating flow						
0	∞	∞	0	0	0	0
−0.025	1.723	1.772	0.292	0.292	0.107	0.110
−0.05	0.967	1.001	0.451	0.447	0.159	0.162
−0.075	0.640	0.613	0.595	0.603	0.204	0.209
−0.10	0.340	0.315	0.786	0.794	0.250	0.254
Separation point						
−0.1168	0	...	1.117	...	0.286	...
−0.120	...	0	...	1.110	...	0.290
Accelerating flow						
+0.025	2.360		0.256		0.098	
0.05	1.893		0.342		0.134	
0.075	1.724		0.398		0.158	
0.100	1.646		0.438		0.176	

Then

$$\phi = U_0x + (ax^2/2) \tag{54a}$$

and

$$p = p_0 - \rho a\phi \tag{54b}$$

From Eq. (17), the outer solution reduces to

$$(u/U_a)^2 = \text{erf}z + \{1-[1/(1+x^*)^2]\}2z(i\text{erfc}z) \tag{55}$$

where $i\text{erfc}z$ is the first repeated integral of the complementary error function [Eqs. (17b) and (17c)].

Setting $z_1 = 0.15$ and $x = 0$ ($x^* = 0$), Eq. (26) gives the value $C = 0.807$. The polynomial inner solution is used for values of $x^* \geqslant -0.05$. For calculations at values of $x^* < -0.05$, the inflection point of the velocity profile ($\partial^2u/\partial y^2 = 0$) was found to occur at values of $z > 0.15$, and hence the von Kármán-Millikan inner solution was used. Nondimensionalized values of shear stress, displacement thickness, and momentum thickness are given in Table 1 for both accelerating ($x^* > 0$) and decelerating ($x^* < 0$) flow. In each case the flow is assumed to have zero initial boundary layer thickness (at $x = 0$). For comparison, exact solution values obtained by Howarth[5] for decelerating flow also are shown.

Some representative velocity profiles are presented in Fig. 2, together with velocity profiles from the exact solution of

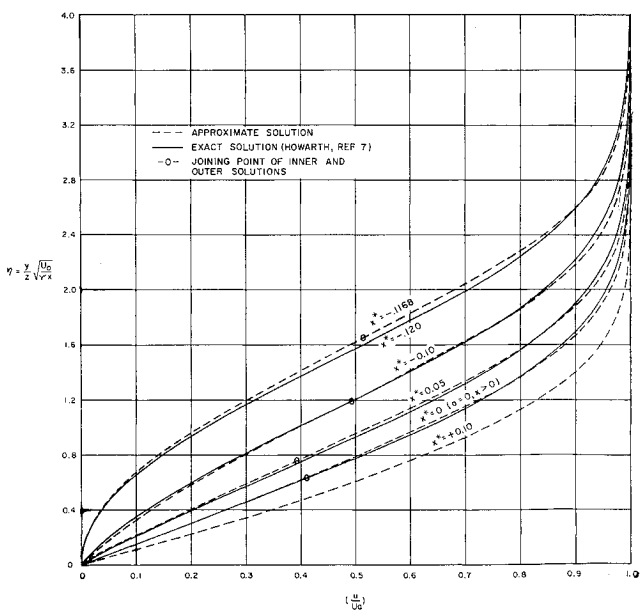

Fig. 2 Velocity profiles for linear variation of stream velocity; $U_a = U_0 + ax = U_0(1 + x^*)$

Table 2 Results for flat plate

	$\frac{\tau_0}{\rho U_a^2}\left(\frac{U_a x}{\nu}\right)^{1/2}$	$\delta^*\left(\frac{u_a}{\nu x}\right)^{1/2}$	$\theta\left(\frac{u_a}{\nu x}\right)^{1/2}$
$z_1 = 0.15$, $C = 0.807$	0.325	1.71	0.645
Blasius	0.332	1.729	0.664
Pohlhausen	0.343	1.752	0.686

Ref. 5 for decelerating flow. Agreement is good right up to the separation point, although separation is predicted at $x^* = -0.1168$, which is slightly earlier than the exact solution value of $x^* = -0.120$. For comparison, the original von Kármán-Millikan method predicts separation at $x^* = -0.102$ and the Pohlhausen integral method at $x^* = -0.151$. It may be noted that a modification of the Pohlhausen method has been developed using seventh-degree velocity profiles for the specific purpose of accurately predicting the separation point.[14] This method predicts separation at $x^* = -0.122$.

The velocity profile shown for $x^* = 0$ is for the special case $a = 0$ (and $x > 0$) corresponding to flow on a flat plate. For this case, the outer solution [Eq. (55)] reduces to

$$(u/U_a)^2 = \text{erf}z \tag{56}$$

and the exact solution reduces to that developed by Blasius. A comparison of nondimensionalized values of τ_0, δ^*, and θ is presented in Table 2, together with values obtained with the Blasius solution and the Pohlhausen integral method. Agreement of all quantities is good and somewhat better than that of the Pohlhausen integral method.

If one considers the special case $U_0 = 0$, $a > 0$ ($x^* = +\infty$) corresponding to flow at a two-dimensional stagnation point, the outer solution [Eq. (55)] becomes

$$(u/U_a)^2 = \text{erf}z + 2z(i\text{erfc}z) \tag{57a}$$

$$= 1 - 4i^2\text{erfc}z \tag{57b}$$

Setting $z = 0.15$, Eq. (26) gives $C = 0.788$. The polynomial inner solution is used for this case ($\partial^2 u/\partial y^2 < 0$ for all z). Values of shear stress, displacement thickness, and momentum thickness are given in Table 3, along with corresponding values obtained from the Pohlhausen integral method and an exact solution of the Navier-Stokes equation (Chap. 5 of Ref. 1). The velocity profile is shown in Fig. 3. Agreement again is seen to be good and somewhat better than the Pohlhausen integral method.

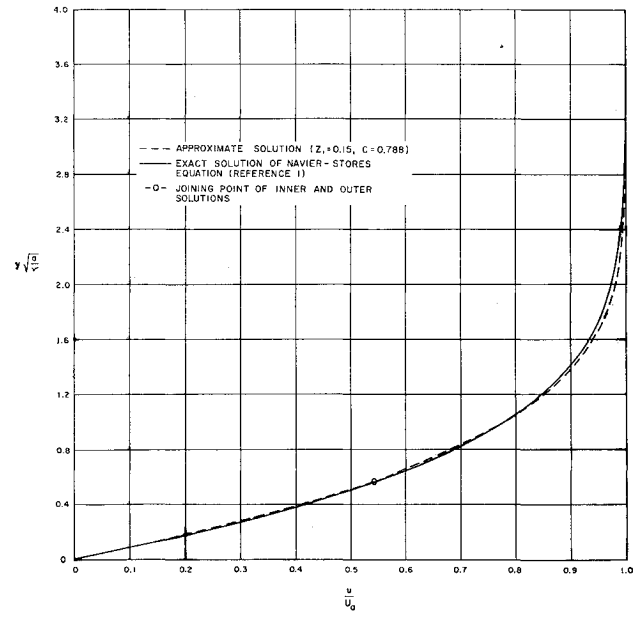

Fig. 3 Velocity profiles for two-dimensional stagnation point flow; $U_a = ax$

Table 3 Results for two-dimensional stagnation point

	$\frac{\tau_0}{\rho U_a^2}\left(\frac{U_a x}{\nu}\right)^{1/2}$	$\delta^*\left(\frac{U_a}{\nu x}\right)^{1/2}$	$\theta\left(\frac{U_a}{\nu x}\right)^{1/2}$
$z = 0.15$, $C = 0.788$	1.223	0.641	0.284
Exact solution	1.233	0.648	0.292
Pohlhausen method	1.19	0.641	0.278

Sinusoidal Variation in Velocity

Consider the case

$$U_a = 2U_\infty \sin(x/R) \tag{58}$$

which is the *inviscid* velocity distribution for two-dimensional flow, at a freestream velocity U_∞, past a circular cylinder of radius R. An "exact" solution based on a method of series expansion has been developed for this velocity distribution (Chap. 9 of Ref. 1). It should be noted that the actual velocity distribution on a circular cylinder is quite different from that of (58) and in effect constitutes a different problem (see next section). Then

$$\phi = 2U_\infty R[1 - \cos(x/\text{R})] \tag{59a}$$

and

$$p = g_0 - (2\rho U_\infty/R)\phi + (\rho/2R^2)\phi^2 \tag{59b}$$

From Eq. (17), the outer solution reduces to

$$\left(\frac{u}{U_a}\right)^2 = \frac{2\cos\eta}{(1+\cos\eta)}(1 - 4i^2\text{erfc}z) + \frac{(1-\cos\eta)}{(1+\cos\eta)}\left[1 - \frac{2}{3}\text{erfc}z + \frac{(2z^2-1)}{3}4i^2\text{erfc}z\right] \tag{60}$$

where $\eta = x/R$ is the meridian angle measured from the forward stagnation point.

Setting $z_1 = 0.15$ and $x = 0$ ($\eta = 0$), Eq. (60) reduces to the outer solution for two-dimensional stagnation point flow (57b), and Eq. (26) gives $C = 0.788$. Resulting nondimensionalized values of τ_0, δ^*, and θ are given in Table 4, and some representative velocity profiles are shown in Fig. 4. The corresponding exact solution is based on a series expansion method described in Ref. 1, Chap. 9, in which the equation for stream velocity (58) is replaced by an eleventh-order polynomial in x. The values shown differ slightly from those of Ref. 1 and were obtained from information supplied in Ref. 10. Although labeled "exact," it should be noted that the values shown for τ_0, δ^*, and θ do not satisfy the boundary layer momentum integral equation in the region of decelerating flow, indicating that a higher-order polynomial is required in order for the series expansion method to be valid in this region.

As shown in Table 4 and Fig. 4, there is close agreement between the approximate and exact solution in the region of accelerating flow ($0 \leqslant \eta \leqslant 90°$) but some discrepancy in the region of decelerating flow ($\eta > 90°$). A part of this discrepancy may be attributed to errors in the "exact" solution.

Circular Cylinder (Hiemenz Velocity Distribution)

The actual velocity distribution on a circular cylinder differs considerably from that of Eq. (58). The velocity distribution observed experimentally by Hiemenz may be expressed by the relation (Ref. 11, p. 150, different units)

$$(U_a/U_\infty) = 3.1657 \times 10^{-2}\eta - 1.4383 \times 10^{-6}\eta^3 - 7.6247 \times 10^{-11}\eta^5 \tag{61}$$

where η is the meridian angle measured from the forward stagnation point in degrees.

For this distribution, the numerical form of the outer solution was used [Eq. (18)], with p being given in terms of g_0 by

Table 4 Results for sinusoidal velocity distribution

$\eta°$	$\frac{\tau_0}{\rho U_\infty^2}\left(\frac{U_\infty R}{\nu}\right)^{1/2}$ Approx.	Exact	$\delta^*\left(\frac{U_\infty}{\nu R}\right)^{1/2}$ Approx.	Exact	$\theta\left(\frac{U_\infty}{\nu R}\right)^{1/2}$ Approx.	Exact
0	0	0	0.456	0.46	0.203	0.21
30	1.62	1.64	0.481	0.49	0.212	0.22
60	2.22	2.26	0.580	0.59	0.250	0.26
90	1.26	1.35	0.918	0.89	0.357	0.35
100	0.34	0.71	1.372	1.12	0.443	0.40
102.45 (separation)	0	...	1.758	...	0.472	...
108.8 (separation)	...	0	...	1.45	...	0.40

Eq. (7a) and $C = 0.788$ from Eq. (26) at the stagnation point.

The resulting nondimensionalized values of τ_0 are given in Table 5, together with values obtained from the relatively accurate numerical procedure of Ref. 3.

Schubauer's Ellipse

With the exception of flow on a flat plate, the only good experimental data on incompressible two-dimensional laminar boundary layer velocity profiles seem to be those obtained by Schubauer in 1935[12] for flow past an ellipse having a ratio of major to minor axis of 2.960 and with major axis aligned with freestream velocity.

The experimental pressure distribution for this ellipse has been used by many investigators to check proposed approximate and exact calculation procedures. One of the most accurate calculations is that due to Hartree.[4] Hartree analyzed the limited number of observed values of pressure reported by Schubauer and arrived at a fairly complete pressure and pressure gradient distribution.

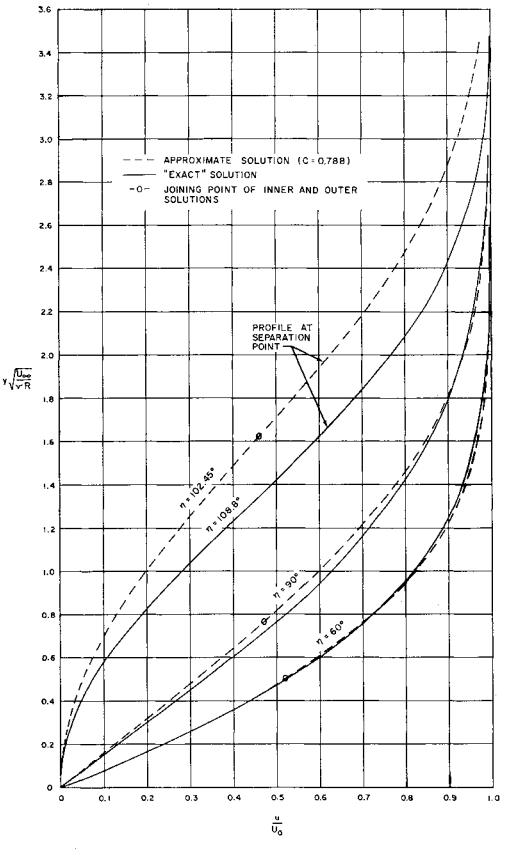

Fig. 4 Velocity profiles for sinusoidal velocity distribution; $U_a = 2U_\infty \sin\eta$ with $\eta = (180/\pi)(x/R)$ deg

Table 5 Shear stress on circular cylinder

$\eta°$	$\frac{\tau_0}{\rho U_a^2}\left(\frac{U_a x}{\nu}\right)^{1/2}$ Approx.	Ref. 3
0	1.223	...
10	1.208	1.228
20	1.201	1.212
30	1.168	1.183
40	1.115	1.134
50	1.038	1.054
60	0.901	0.920
70	0.638	0.675
78.13 (separation)	0	...
80 (separation)	...	0

Using Hartree's interpretation of the data, the numerical form of the outer solution was used [Eq. (19)], with $C = 0.788$ from Eq. (26), for $z_1 = 0.15$ at the stagnation point. Some resulting nondimensionalized values of τ_0, δ^*, and θ are shown in Table 6, together with Hartree's values. The minor axis is used as the reference length L.

As shown in Table 6, the approximate solution gives good agreement with Hartree's fairly rigorous numerical calculation. It may be noted that neither solution predicts flow separation ($\tau_0 = 0$), whereas Schubauer observed separation to occur at $x/L = 1.99 \pm 0.02$. Another relatively rigorous numerical calculation presented in Ref. 3 also fails to show flow separation. All three solutions are close to separation in the vicinity of the observed separation point, however, and can be made to show separation with small changes in the pressure distribution. Howarth[5] has noted that the boundary layer at the observed separation point may not have been thin enough for the approximations of boundary layer theory to be valid. Whatever the reason, the most rigorous calculation procedures fail to predict flow separation for this problem.

Three representative velocity profiles are shown in Fig. 5. Station $x/L = 0.545$ is in a region of accelerating flow, station $x/L = 1.457$ is just aft of the minimum pressure station, and station $x/L = 1.946$ is just ahead of the separation point. There is good agreement with the experimental profiles in all three cases.

Concluding Remarks

The procedure outlined in this paper occupies a middle ground between the integral method and numerical methods, with respect to accuracy and computing time. A typical problem involving calculation of velocity profiles τ_0, δ^*, and θ for 7 to 10 stations takes from 2 to 5 min on an IBM 7090 digital computer.

The method differs from that of von Kármán-Millikan[6] in having the constant C in the outer solution and in the use of a polynomial inner solution for all but highly inflected velocity

Table 6 Results for Schubauer's ellipse

$\frac{x}{L}$	$\frac{2\tau_0}{\rho U_\infty^2}\left(\frac{U_\infty L}{\nu}\right)^{1/2}$ Approx.	Hartree	$\frac{\delta^*}{L}\left(\frac{U_\infty L}{\nu}\right)^{1/2}$ Approx.	Hartree	$\frac{\theta}{L}\left(\frac{U_\infty L}{\nu}\right)^{1/2}$ Approx.	Hartree
0.2	3.55	3.69	0.391	0.37	0.165	0.16
0.4	2.56	2.60	0.618	0.61	0.253	0.25
0.6	1.96	2.02	0.820	0.808	0.329	0.331
0.8	1.58	1.64	1.00	0.993	0.397	0.402
1.0	1.29	1.34	1.19	1.177	0.462	0.468
1.2	1.09	1.12	1.37	1.354	0.524	0.531
1.4	0.90	0.94	1.56	1.537	0.587	0.592
1.6	0.61	0.69	1.86	1.794	0.662	0.664
1.8	0.35	0.40	2.29	2.194	0.751	0.748
1.9	0.22	0.26	2.60	2.472	0.801	0.799
2.0	0.17	0.19	2.82	...	0.846	...

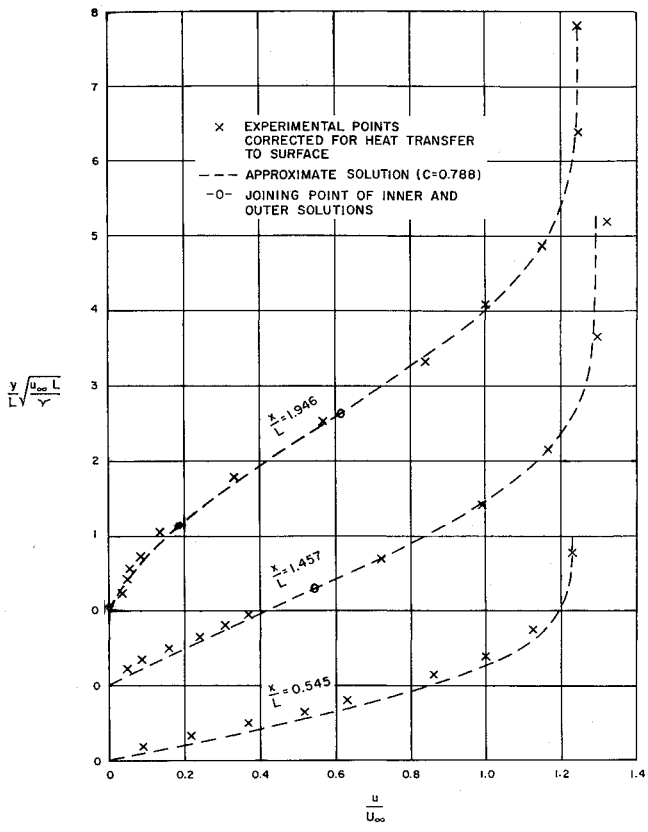

Fig. 5 Velocity profiles for Schubauer's ellipse

profiles. The notation and the form in which the inner and outer solutions are presented differ considerably from that of Ref. 6, and it is hoped that the present form is somewhat easier to follow. With respect to notation, the equations have, for the most part, been left in terms of dimensional quantities primarily because each problem seems to lend itself to a slightly different nondimensional form.

The method may be extended to a restricted class of compressible flows (perfect gas flow past an adiabatic wall with viscosity proportional to absolute temperature) by means of the Stewartson transformation and to axisymmetric flow by means of the Mangler transformation.

References

[1] Schlichting, H., *Boundary Layer Theory* (McGraw-Hill Book Co. Inc., New York, 1960), 4th ed.

[2] Pai, S. I., *Viscous Flow Theory* (D. Van Nostrand Co. Inc., New York, 1956), Vol. 1, Chap. 8–10.

[3] Smith, A. M. O. and Clutter, D. W., "Solution of the incompressible laminar boundary layer equations," Douglas Aircraft Co. Inc., Rept. ES40446 (1961).

[4] Hartree, D. R., "The solution of the equations of the laminar boundary layer for Schubauer's observed pressure distribution for an elliptic cylinder," British Aeronaut. Research Council RM2427 (1949).

[5] Howarth, L., "On the solution of the laminar boundary layer equations," Proc. Roy. Soc. (London) **164A**, 547 (1938).

[6] von Kármán, T. and Millikan, C. B., "On the theory of laminar boundary layer involving separation," NACA TR 504 (1934).

[7] Nash, J. F., "Laminar mixing of a non-uniform stream with a fluid at rest," British Aeronaut. Research Council, no. 22, 245 (September 1960).

[8] Carslaw, H. S. and Jaeger, J. C., *Conduction of Heat in Solids* (Oxford University Press, London, 1959), 2nd ed., Appendix II.

[9] Millikan, C. B., "A theoretical calculation of the laminar boundary layer around an elliptic cylinder, and its comparison with experiment," J. Aeronaut. Sci. **3**, 91–94 (1936).

[10] Schlichting, H., private communication (March 28, 1962).

[11] Goldstein, S., *Modern Developments in Fluid Dynamics* (Oxford University Press, London, 1938), Vol. 1, p 150.

[12] Schubauer, G. B., "Air flow in a separating laminar boundary layer," NACA Rept. 527 (1935).

[13] Lewis, J. A. and Carrier, G. F., "Some remarks on the flat plate boundary layer," Quart. Appl. Math. **7**, 228–234 (1949.)

[14] Morduchow, M., "Analysis and calculation by integral methods of laminar compressible boundary layer with heat transfer and with and without pressure gradient," NACA Rept. 1245 (1955).